JOURNAL OF BACTERIOLOGY, June 2007, p. 4305–4309 Vol. 189, No. 11
0021-9193/07/$08.00+0 doi:10.1128/JB.00042-07
Copyright © 2007, American Society for Microbiology. All Rights Reserved.

NOTES

Flagellar Motility and Structure in the Hyperthermoacidophilic Archaeon *Sulfolobus solfataricus*▽

Zalán Szabó,[1]† Musa Sani,[2] Maarten Groeneveld,[1]‡ Benham Zolghadr,[1] James Schelert,[3] Sonja-Verena Albers,[1] Paul Blum,[3] Egbert J. Boekema,[2] and Arnold J. M. Driessen[1]*

Department of Microbiology, Groningen Biomolecular Sciences and Biotechnology Institute, University of Groningen, Kerklaan 30, 9751 NN Haren, The Netherlands[1]; Department of Biophysical Chemistry, Groningen Biomolecular Sciences and Biotechnology Institute, University of Groningen, Nijenborgh 4, 9747 AG Groningen, The Netherlands[2]; and Beadle Center for Genetics, University of Nebraska, Lincoln, Nebraska 68588-0666[3]

Received 9 January 2007/Accepted 25 March 2007

Flagellation in archaea is widespread and is involved in swimming motility. Here, we demonstrate that the structural flagellin gene from the crenarchaeaon *Sulfolobus solfataricus* is highly expressed in stationary-phase-grown cells and under unfavorable nutritional conditions. A mutant in a flagellar auxiliary gene, *flaJ*, was found to be nonmotile. Electron microscopic imaging of the flagellum indicates that the filaments are composed of right-handed helices.

The ability of organisms to actively change location can greatly increase their chances of survival in an ever-changing environment. Bacteria achieve this in numerous ways, of which the best-studied examples are swimming motility driven by rotating flagella and twitching motility mediated by retractable type IV pili (8). In archaea, flagella are also responsible for swimming motility. However, the structural subunits (flagellins) assemble into a filament that is more reminiscent of type IV pili. Both type IV pilins and archaeal flagellins are synthesized as precursors with a conserved type IV pilin-like signal sequence at the N terminus. The positively charged leader peptide of the signal sequence is cleaved off by a signal peptidase, while the adjacent hydrophobic domain remains a part of the mature protein (4, 6, 36). Structural studies of type IV pili and the flagellar filament from *Halobacterium salinarum* provided additional evidence for the relatedness of these cell appendages. Both are thin right-handed helical filaments (6 to 9 nm and approximately 10 nm in diameter, respectively) with a central hydrophobic core comprised of the conserved N-terminal α-helix of pilin and, most likely, also flagellin subunits (14–16, 40). Swimming motility has so far been demonstrated for several euryarchaea and the crenarchaeon *Sulfolobus acidocaldarius* by direct microscopical observation or indirectly as a swarming phenotype on semisolid agar plates. In *H. salinarum* and *Methanococcus voltae*, motility was shown to be dependent on the flagellar filaments comprised of the structural FlaB proteins (1, 9, 22, 25, 27, 35).

Three components of archaeal flagellar biogenesis are related to proteins involved in type IV pilus assembly: the preflagellin peptidase (FlaK in *Methanococcus maripaludis* [6] and PibD in *Sulfolobus solfataricus* [4]), the type II/IV secretion system ATPase homolog FlaI, and the polytopic membrane protein FlaJ. The accessory genes encoding these proteins are required for flagellum biogenesis in *M. voltae* (7, 39). Additionally, an *H. salinarum flaI* mutant lacking flagella was nonmotile (31). In analogy with the type IV pilus systems, FlaI and FlaJ are assumed to constitute the core of the machinery that assembles flagella (5, 32). In most cases, the genes coding for flagellins (*flaA* and *flaB*) colocalize with accessory genes in the genome (37).

So far, the emphasis of archaeal flagella research has been on organisms belonging to the *Euryarchaeota* and little is known about flagella in the *Crenarchaeota*, the other main archaeal phylum (19, 20, 25). Flagella have previously been isolated only from *Sulfolobus shibatae* (19). This report describes a study of the flagellar system of the thermoacidophilic crenarchaeon *Sulfolobus solfataricus*, including the generation of an *flaJ* knockout strain that is nonmotile.

Analysis of the *fla* gene locus in *Sulfolobus solfataricus*. The flagellum operon of the sequenced *S. solfataricus* P2 strain is disrupted by an insertion sequence (IS) element integrated into the coding region of the *flaG* gene (SSO2321 [34]). However, PCR analysis of the gene region suggested that this integration is not stable under laboratory growth conditions, as we frequently observed flagellated *S. solfataricus* P2 cells (Fig. 1B). Additionally, this IS element is completely absent in a related strain, *S. solfataricus* PBL2025 (an *S. solfataricus* 98/2 derivative [21]), as determined by PCR amplification and sequence analysis of the *flaG* gene (data not shown). The coding

* Corresponding author. Mailing address: Department of Microbiology, Groningen Biomolecular Sciences and Biotechnology Institute, University of Groningen, Kerklaan 30, 9751 NN Haren, The Netherlands. Phone: 31-50-3632164. Fax: 31-50-3632154. E-mail: a.j.m.driessen@rug.nl.

† Present address: Institute of Enzymology, Hungarian Academy of Sciences, Karolina út 29, 1113 Budapest, Hungary.

‡ Present address: Department of Biochemistry, Groningen Biomolecular Sciences and Biotechnology Institute, University of Groningen, Nijenborgh 4, 9747 AG Groningen, The Netherlands.

▽ Published ahead of print on 6 April 2007.

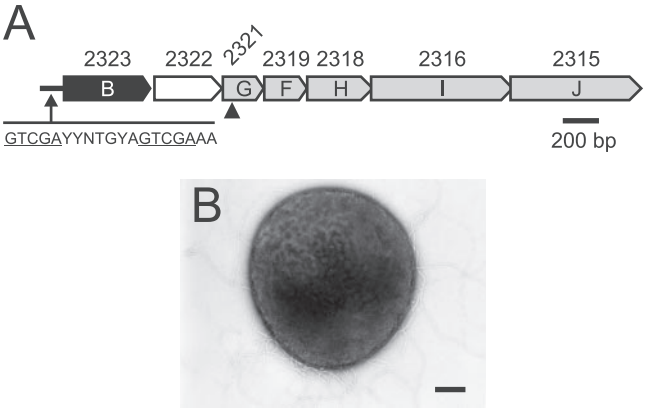

FIG. 1. Genomic organization of the *fla* operon and flagellation of *S. solfataricus* P2. (A) Schematic representation of the *S. solfataricus fla* operon. An IS element disrupted the SSO2321 gene in the sequenced P2 strain (insertion site indicated by an arrowhead) but is absent in PBL2025. Genes are shown as open arrows with gene designations based on homology. The structural flagellin gene is in black, and genes with predicted accessory functions are gray. Suffixes of *fla* genes with identified homologies are depicted in the boxes, while locus tag (SSO) numbers are given above the boxes. SSO2322 (white arrow) is so far unique to the genus *Sulfolobus*. A conserved 5-base direct repeat (underlined), starting 75 bases upstream of the translational start site of *flaB*, is shown. The consensus sequence was derived from an alignment of *flaB* promoter sequences from three sequenced *Sulfolobus* species. Nucleotide base codes are as follows: Y, C or T; N, any nucleotide. (B) Transmission electron microscopy image of a negatively stained flagellated cell of *S. solfataricus* P2. Bar, 200 nm.

sequences of the *flaG* gene were identical in both *S. solfataricus* strains at the nucleotide level. The flagellum (*fla*) operon encodes seven open reading frames (Fig. 1A), one structural protein (FlaB), five putative accessory proteins (FlaGFHIJ), and one open reading frame (SSO2322) for which homologs can be found only in the other two available *Sulfolobus* genomes (12, 23). The last open reading frame is not homologous to any known flagellar accessory protein but contains a putative coiled-coil domain. To find conserved regions within the *flaB* promoter, sequences upstream of *flaB* genes obtained from the three available *Sulfolobus* sp. genome sequences were aligned using ClustalW (13). A 5-base-pair direct repeat was detected, starting 75 bases upstream of the translational start site and 30 bases upstream of a putative TATA box and BRE site. A direct repeat sequence was previously identified upstream of the *flaB1* gene of the methane-producing archaeon *Methanococcus jannaschii*, which could be a transcriptional regulator binding site (38). In this organism, the induction of flagellar protein synthesis was detected at high cell densities and excess hydrogen, or low hydrogen, partial pressure (28).

Transcriptional regulation of the *flaB* gene. We aimed to find conditions under which the flagellin gene is highly induced. Northern blot analysis was performed on RNA isolated from *S. solfataricus* P2 cells (obtained from DSMZ, Braunschweig, Germany) grown under different conditions, using part of the *flaB* gene as a probe. Cells were grown aerobically at 80°C and pH 3 in Brock's basal salt medium (minimal medium [MM]) (11). This medium was supplemented with either 0.2% tryptone (Difco), 0.1% yeast extract, and 0.2% sucrose (rich medium), or 0.2% sugar (glucose or arabinose). For analysis of *flaB* gene transcript levels, 5 μg of isolated total RNA (3) was separated on a denaturing 1.1% agarose gel and subsequently capillary blotted onto Zeta-Probe membranes (Bio-Rad). Nonradioactive hybridization and detection were performed as described previously (24). First, early and late growth phases of cells grown in rich medium were compared. While little *flaB* transcript was detected in samples from the mid-logarithmic growth phase, a strong induction in stationary cells was observed (Fig. 2B). We were unable to correlate the increased levels of *flaB* transcript to elevated amounts of flagella by electron microscopy. Log-phase-grown cells do contain flagella, while stationary-phase-grown cells could not be investigated by electron microscopy because they are highly prone to lysis (data not shown).

The induction might be due to a limitation of nutrient availability or a possible quorum-sensing mechanism (17). No homologs of bacterial quorum-sensing systems have been detected in archaea so far (10), although quorum sensing seems to exist as shown for the induction of an extracellular protease in *Natronococcus occultus* (30). To determine whether unfavorable nutritional conditions induce *flaB* expression, cells were shifted from rich medium to MM and samples were taken for Northern analysis. A cell culture grown in rich medium to mid-logarithmic phase was collected by centrifugation and resuspended in either rich medium or MM without the addition of a carbon source. Samples were taken before and 1 and 2 hours after the shift and analyzed as described above (Fig. 2A). No change in *flaB* transcript was observed when cells continued to grow on rich medium. However, a strong induction could be detected after 2 hours of incubation in MM. The up-regulation of *flaB* was confirmed by semiquantitative reverse transcriptase (RT) PCR performed on RNA isolated from cells grown under the conditions described above (Fig. 2B and C). RT-PCR was performed as described previously (3) with primers flaB1 (5′-AGACAGCGTCAACAGACTA-3′) and flaB2 (5′-ACCTGCACTTGTCTGCTGAT-3′). The absence of DNA contamination in all RNA preparations was confirmed by performing PCRs without prior reverse transcription (not shown). In addition, increased amounts of *flaB* transcript were detected in cells grown on sugars (glucose or arabinose) compared to that in cells grown with peptides (tryptone) or on rich medium (Fig. 2D). As peptide carbon sources are preferred over sugar MM conditions by *S. solfataricus* (26), the flagellin gene seems to be preferentially expressed in cells that are exposed to unfavorable nutritional conditions.

Construction and characterization of an *flaJ* disruption mutant. To determine whether the *flaJ* accessory gene is involved in flagellar biogenesis and motility in *S. solfataricus*, a disruption mutant was constructed in strain PBL2025. *S. solfataricus* PBL2025 contains a large chromosomal deletion which also includes *lacS*, the gene coding for β-glycosidase, and accordingly, these cells are not able to grow on lactose as the sole carbon source (33). The *flaJ* gene was targeted using a suicide plasmid (pET2275) carrying the *flaJ* coding region interrupted at base 685 by the *lacS* gene as a selectable marker (Fig. 3A). The *lacS* gene with its own promoter and terminator region was cloned by PCR amplification (using primers with the sequences 5′-CCCCCCATGGCTCCTCTTATTATTAGAATT GTACGC-3′ and 5′-CCCCCGGATCCCTAGTGTTGCAAG GCAG-3′; NcoI and BamHI restriction sites are underlined,

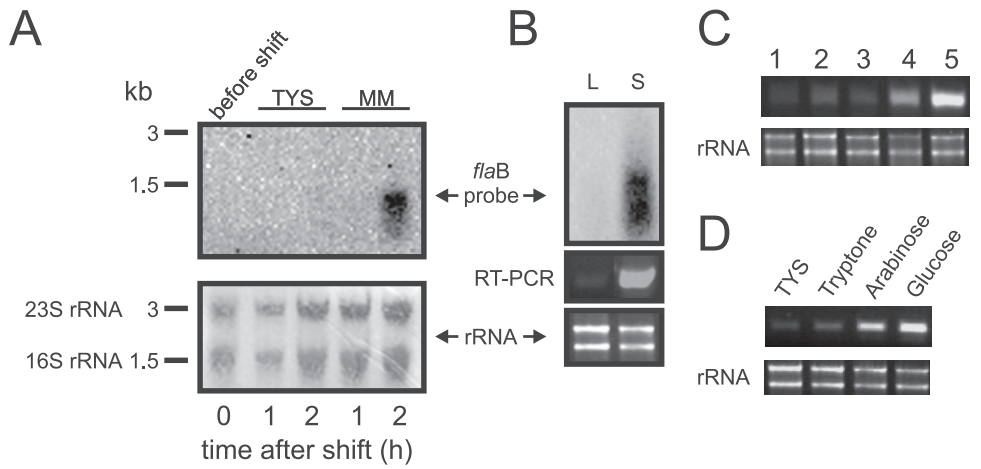

FIG. 2. Transcriptional regulation of *flaB* tested in *S. solfataricus* strain P2. (A) Northern analysis of *flaB* gene transcript after transfer of a cell culture from rich medium (TYS) to MM. RNA was isolated from cells before and 1 and 2 hours after the shift into either rich medium or MM. The *flaB* gene transcript was detected using a specific digoxigenin-labeled probe (top). The positions of the 16S and 23S ribosomal RNAs, determined by methylene blue staining of the blot membrane (bottom), are indicated. (B) Detection of *flaB* gene transcript levels at different growth stages by Northern analysis (top) and RT-PCR (middle). RNA was isolated from cells grown in rich medium to mid-logarithmic (L) or stationary (S) phase. Amounts of RNA identical to those used in the Northern blot analysis were separated on 1.5% agarose gels and stained with ethidium bromide (bottom). (C and D) Semiquantitative RT-PCR analysis of *flaB* expression levels in *S. solfataricus* cells either transferred from rich medium to MM (C) or grown on MM supplemented with a carbon source as indicated and harvested at an optical density of 0.6 (D). Samples for panel C were taken under conditions identical to those described for panel A. The upper panels show the PCR products, and the lower panels are a loading control for the RNA used in the RT-PCRs.

respectively), with *S. solfataricus* P2 genomic DNA as a template. The PCR product was ligated into NcoI- and BamHI-cut pET401 cloning vector (K. H. M. van Wely, unpublished data), yielding pET2268, and the endogenous EcoRV site of *lacS* was subsequently removed by site-directed mutagenesis (43). The N-terminal (673 bp) and C-terminal (728 bp) coding regions of *flaJ* were amplified by PCR using primers with the sequences 5′-CCCCGGTACCGCAAAAAATGAAGTAGACTC C-3′ and 5′-CCCCCCATGGCGATTCCTAATAGAACTA TACCAG-3′ (KpnI and NcoI restriction sites are underlined, respectively) and 5′-CCCCGGATCCAGGTATAGATTGTA TGAAAAT-3′ and 5′-CCCCCGCGGCCGCGTAATAAACC CGATGGTGATGC-3′ (BamHI and NotI restriction sites are underlined, respectively), respectively, with *S. solfataricus* P2 genomic DNA as a template. The cut PCR products were inserted into pET2268 by using the appropriate restriction enzymes, resulting in pET2275. After electroporation of *S. solfataricus* PBL2025 with pET2275, a strain carrying the integrant was selected on liquid MM supplemented with lactose and purified as described before (43). The integrity of the mutant was confirmed by PCR amplification of part of the *flaJ* gene region (Fig. 3A and B). As expected, using DNA from the wild-type strain as a template and primers flaJ1 (5′-GCTCCC TTACCTTTCTAGTAGC-3′) and flaJ2 (5′-GCCTTACGTCT CCTAGATCC-3′), a 428-base-pair fragment was amplified (Fig. 3B). A PCR performed on DNA isolated from the *flaJ*::*lacS* strain with the same primers resulted in a larger fragment of 2.4 kb corresponding to the *flaJ* gene carrying the *lacS* insert (Fig. 3B). Also, the two regions overlapping the *flaJ* flanks and the selection marker were amplified by PCR and analyzed by direct sequencing of the PCR products. The resulting *flaJ*::*lacS* mutant strain and the wild-type strain were characterized for motility and the presence of flagella. Cells grown in liquid glucose medium were negatively stained with 2% uranyl acetate and examined by transmission electron microscopy (Fig. 3C and D). Cells of the wild-type strain appeared to be peritrichous, without any bundling of filaments (Fig. 3C). Flagella were usually short with a slight wave-like curvature. Longer filaments of up to several micrometers in length were also observed. On the other hand, cells of the *flaJ* strain completely lacked flagella on the cell surface (Fig. 3D). To establish whether flagella conferred motility in *S. solfataricus*, a swarming assay on semisolid plates was established. To prepare semisolid medium, 0.2% Gelrite (Serva, Heidelberg, Germany), dissolved by stirring in boiling demineralized water, was added to an equal volume of two-times-concentrated MM containing 0.02% glucose and 20 mM magnesium chloride and 6 mM calcium chloride as solidifying agents. The pH of the medium was adjusted to 3. To inoculate the plates, cells grown on MM supplemented with 0.1% glucose were pelleted (10 min, 3,500 × *g*, 21°C) and resuspended in 0.1 volume of culture supernatant. Next, a 10-μl droplet of this suspension, corresponding to approximately 10^7 cells, was applied to the center of the plate and allowed to absorb into the medium. Plates were incubated for 5 to 6 days in a sealed humid chamber at 80°C. Strain PBL2025 formed a dense circular spot of cells, corresponding to the area of inoculation, and a lighter halo around this region, consistent with a swarming phenotype (Fig. 3E). In contrast, no halo formation was observed with the *flaJ* cells (Fig. 3F). Therefore, the *flaJ* gene product is required for the biogenesis of flagella on *S. solfataricus* cells as well as for swarming motility. FlaJ is the only polytopic membrane protein in the *fla* operon, and based on its similarity to bacterial GspF proteins, it is tempting to speculate that it constitutes the platform on which the flagellum is assembled in the cytoplasmic membrane by the ATPase FlaI (3).

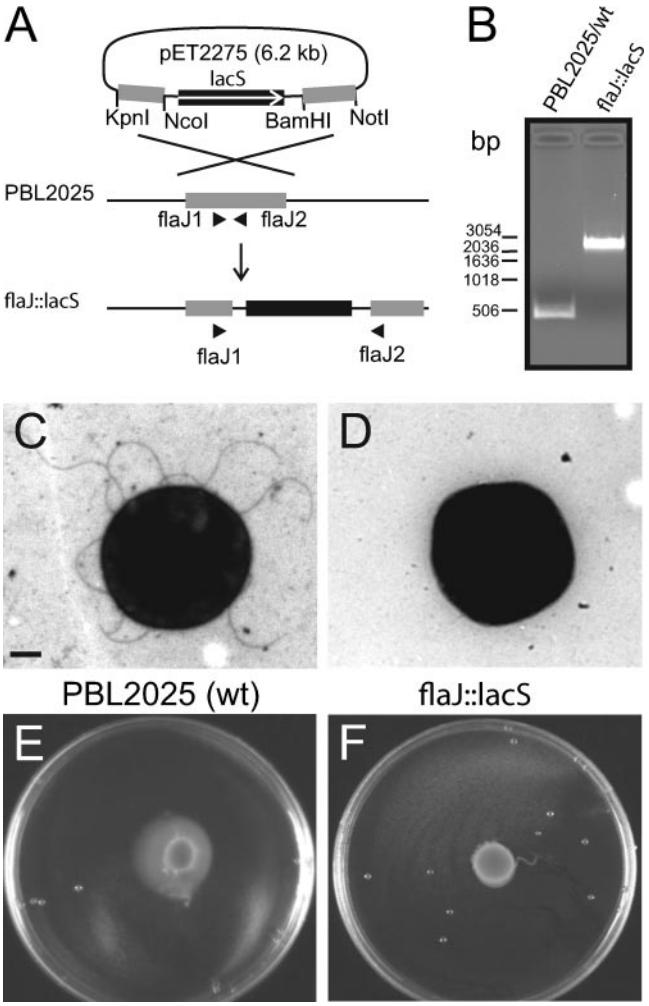

FIG. 3. Construction of an *flaJ* disruption mutant and characterization of wild-type versus mutant strains. (A) Schematic representation of the genomic environment of the *flaJ* gene and the suicide plasmid used to target the gene. Arrowheads indicate primers flaJ1 and flaJ2. The recognition sites of selected restriction enzymes on the genomic fragment are HindIII, EcoRI, and ScaI. (B) Results of a PCR on genomic DNA isolated from strain PBL2025-*flaJ*::*lacS* or strain PBL2025 (wild type [wt]). (C and D) Transmission electron microscopy images of negatively stained cells. Bar, 200 nm. (E and F) Motility was assayed on semisolid Gelrite plates supplemented with MM plus 0.05% glucose.

Structural features of isolated flagella. *Sulfolobus* species carry only one copy of the flagellin gene (4, 34) and do not show reversed swimming or tumbling (20, 25). Therefore, we argued that the structure of flagella from this organism should be homogenous, in contrast to polymorphic flagella from *H. salinarum* that are built up of multiple subunits (40). To obtain structural information about the flagellar filament, a series of electron micrographs was collected for negatively stained specimens isolated from culture supernatants. A crude flagellar preparation was isolated from culture supernatants of *S. solfataricus* PBL2025 grown in MM supplemented with 0.1% glucose until stationary phase. Cells were removed by centrifugation (30 min, 3,000 × *g*, 4°C). The supernatant was recentrifuged, and the resulting culture supernatant was pelleted by

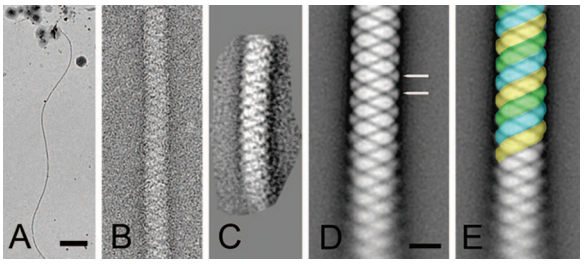

FIG. 4. Electron microscopy analysis of the *S. solfataricus* flagellum. (A) Example of a long flagellar filament showing a typical wavelike pattern. (B) A typical segment of a flagellum, used for image processing; the helical motif of the filament is readily recognizable. (C) The projection average of 33 aligned metal-shadowed segments indicates that the filament is right-handed. (D) Two-dimensional projection average of 120 aligned segments. (E) Scheme for the helical packing projected on the averaged image of frame (D). The three-start left-handed helical packing is indicated in color. Bars, 1 μm (A) and 10 nm (D and E).

ultracentrifugation (20 min, 26,000 × *g*, 4°C). This pellet contained numerous flagella as well as cellular debris and was used for initial electron microscopy observations. The centrifugation of the supernatant (45 min, 220,000 × *g*, 4°C) resulted in a pellet which consisted mainly of flagella. This material was used for detailed analysis of the flagellar ultrastructure. Flagellar filament suspensions were negatively stained with 2% uranyl acetate on glow-discharged carbon-coated copper grids. Flagella were observed on a Philips CM120 electron microscope, operating at 120 kV with a LaB6 filament. Images were recorded with a charge-coupled-device camera at ×80,000 magnification with a pixel size of 3.75 Å at the specimen level with GRACE software (29). Long filaments of up to several micrometers extending out of the grid plane were frequently observed (Fig. 4A). Segments of filaments which were rather straight were extracted from micrographs for image analysis (Fig. 4B). A single-particle approach (performed with the Groningen Image Processing software package) was used for processing (18). Slightly overlapping segments were extracted from the micrographs. To correct for the significant in-plane curvature, we first rotationally aligned all segments. The best 60% of the rotationally oriented segments, as judged by using the correlation coefficient as the quality criterion, were then further processed by full alignment procedures. The aligned projections were treated with multivariate statistical analysis in combination with hierarchical classification (41) before final averaging. The final average projection map of 120 segments clearly shows that the filament has a helical packing (Fig. 4D). The filament has a diameter of 145 Å and a pitch of 54 Å (Fig. 4D). Thus, the *S. solfataricus* flagellum is thicker than that of *H. salinarum* (approximately 100 Å) (14), probably due to the higher molecular weight of the *S. solfataricus* flagellin. The filament has an apparent three-stranded helical arrangement, as indicated in the scheme in Fig. 4E. The resolution of the two-dimensional map is about 18 Å. Surface metal shadowing was performed to determine the handedness of the expected helical packing of the filaments (Fig. 4C). The contribution of the helices in one direction, from the lower left to the upper right, was stronger than in the upper-left to lower-right direction (Fig. 4C). This indicated that the filaments are composed

of right-handed helices, as is the case for the flagellum of *H. salinarum* (2, 14).

In this study, we have investigated flagellation in *S. solfataricus* and established a basis for future investigations of cell surface-exposed structures. Because flagella are abundant on *Sulfolobus* cells, the availability of a nonflagellated mutant will significantly ease the investigation of other types of membrane-bound organelles, including pili (42) and the bindosome, a putative assembly of ABC transporter binding proteins involved in the efficient uptake of various sugars (3, 5).

This work was supported by a Van der Leeuw grant to A.J.M.D. from the Earth and Life Sciences Foundation (ALW), which is subsidized by the Dutch Organization for Scientific Research (NWO), and Veni and Vidi grants to S.-V.A. from NWO.

REFERENCES

1. **Alam, M., M. Lebert, D. Oesterhelt, and G. L. Hazelbauer.** 1989. Methyl-accepting taxis proteins in *Halobacterium halobium*. EMBO J. **8:**631–639.
2. **Alam, M., and D. Oesterhelt.** 1984. Morphology, function and isolation of halobacterial flagella. J. Mol. Biol. **176:**459–475.
3. **Albers, S. V., and A. J. M. Driessen.** 2005. Analysis of ATPases of putative secretion operons in the thermoacidophilic archaeon *Sulfolobus solfataricus*. Microbiology **151:**763–773.
4. **Albers, S. V., Z. Szabo, and A. J. M. Driessen.** 2003. Archaeal homolog of bacterial type IV prepilin signal peptidases with broad substrate specificity. J. Bacteriol. **185:**3918–3925.
5. **Albers, S. V., Z. Szabo, and A. J. M. Driessen.** 2006. Protein secretion in the Archaea: multiple paths towards a unique cell surface. Nat. Rev. Microbiol. **4:**537–547.
6. **Bardy, S. L., and K. F. Jarrell.** 2002. FlaK of the archaeon *Methanococcus maripaludis* possesses preflagellin peptidase activity. FEMS Microbiol. Lett. **208:**53–59.
7. **Bardy, S. L., and K. F. Jarrell.** 2003. Cleavage of preflagellins by an aspartic acid signal peptidase is essential for flagellation in the archaeon *Methanococcus voltae*. Mol. Microbiol. **50:**1339–1347.
8. **Bardy, S. L., S. Y. Ng, and K. F. Jarrell.** 2003. Prokaryotic motility structures. Microbiology **149:**295–304.
9. **Black, F. T., E. A. Freundt, O. Vinther, and C. Christiansen.** 1979. Flagellation and swimming motility of *Thermoplasma acidophilum*. J. Bacteriol. **137:**456–460.
10. **Boucher, Y., C. J. Douady, R. T. Papke, D. A. Walsh, M. E. Boudreau, C. L. Nesbo, R. J. Case, and W. F. Doolittle.** 2003. Lateral gene transfer and the origins of prokaryotic groups. Annu. Rev. Genet. **37:**283–328.
11. **Brock, T. D., K. M. Brock, R. T. Belly, and R. L. Weiss.** 1972. *Sulfolobus*: a new genus of sulfur-oxidizing bacteria living at low pH and high temperature. Arch. Mikrobiol. **84:**54–68.
12. **Chen, L., K. Brügger, M. Skovgaard, P. Redder, Q. She, E. Torarinsson, B. Greve, M. Awayez, A. Zibat, H.-P. Klenk, and R. A. Garrett.** 2005. The genome of *Sulfolobus acidocaldarius*, a model organism of the *Crenarchaeota*. J. Bacteriol. **187:**4992–4999.
13. **Chenna, R., H. Sugawara, T. Koike, R. Lopez, T. J. Gibson, D. G. Higgins, and J. D. Thompson.** 2003. Multiple sequence alignment with the Clustal series of programs. Nucleic Acids Res. **31:**3497–3500.
14. **Cohen-Krausz, S., and S. Trachtenberg.** 2002. The structure of the archeabacterial flagellar filament of the extreme halophile *Halobacterium salinarum* R1M1 and its relation to eubacterial flagellar filaments and type IV pili. J. Mol. Biol. **321:**383–395.
15. **Craig, L., M. E. Pique, and J. A. Tainer.** 2004. Type IV pilus structure and bacterial pathogenicity. Nat. Rev. Microbiol. **2:**363–378.
16. **Craig, L., N. Volkmann, A. S. Arvai, M. E. Pique, M. Yeager, E. H. Egelman, and J. A. Tainer.** 2006. Type IV pilus structure by cryo-electron microscopy and crystallography: implications for pilus assembly and functions. Mol. Cell **23:**651–662.
17. **Daniels, R., J. Vanderleyden, and J. Michiels.** 2004. Quorum sensing and swarming migration in bacteria. FEMS Microbiol. Rev. **28:**261–289.
18. **Egelman, E. H.** 2000. A robust algorithm for the reconstruction of helical filaments using single-particle methods. Ultramicroscopy **85:**225–234.
19. **Faguy, D. M., D. P. Bayley, A. S. Kostyukova, N. A. Thomas, and K. F. Jarrell.** 1996. Isolation and characterization of flagella and flagellin proteins from the thermoacidophilic archaea *Thermoplasma volcanium* and *Sulfolobus shibatae*. J. Bacteriol. **178:**902–905.
20. **Grogan, D. W.** 1989. Phenotypic characterization of the archaebacterial genus *Sulfolobus*: comparison of five wild-type strains. J. Bacteriol. **171:**6710–6719.
21. **Haseltine, C., M. Rolfsmeier, and P. Blum.** 1996. The glucose effect and regulation of α-amylase synthesis in the hyperthermophilic archaeon *Sulfolobus solfataricus*. J. Bacteriol. **178:**945–950.
22. **Jarrell, K. F., D. P. Bayley, V. Florian, and A. Klein.** 1996. Isolation and characterization of insertional mutations in flagellin genes in the archaeon *Methanococcus voltae*. Mol. Microbiol. **20:**657–666.
23. **Kawarabayasi, Y., Y. Hino, H. Horikawa, K. Jin-no, M. Takahashi, M. Sekine, S. Baba, A. Ankai, H. Kosugi, A. Hosoyama, S. Fukui, Y. Nagai, K. Nishijima, R. Otsuka, H. Nakazawa, M. Takamiya, Y. Kato, T. Yoshizawa, T. Tanaka, Y. Kudoh, J. Yamazaki, N. Kushida, A. Oguchi, K. Aoki, S. Masuda, M. Yanagii, M. Nishimura, A. Yamagishi, T. Oshima, and H. Kikuchi.** 2001. Complete genome sequence of an aerobic thermoacidophilic crenarchaeon, Sulfolobus tokodaii strain7. DNA Res. **8:**123–140.
24. **Koning, S. M., M. G. Elferink, W. N. Konings, and A. J. M. Driessen.** 2001. Cellobiose uptake in the hyperthermophilic archaeon *Pyrococcus furiosus* is mediated by an inducible, high-affinity ABC transporter. J. Bacteriol. **183:**4979–4984.
25. **Lewus, P., and R. M. Ford.** 1999. Temperature-sensitive motility of *Sulfolobus acidocaldarius* influences population distribution in extreme environments. J. Bacteriol. **181:**4020–4025.
26. **Lubelska, J. M., M. Jonuscheit, C. Schleper, S. V. Albers, and A. J. M. Driessen.** 2006. Regulation of expression of the arabinose and glucose transporter genes in the thermophilic archaeon *Sulfolobus solfataricus*. Extremophiles **10:**383–391.
27. **Marwan, W., M. Alam, and D. Oesterhelt.** 1991. Rotation and switching of the flagellar motor assembly in *Halobacterium halobium*. J. Bacteriol. **173:**1971–1977.
28. **Mukhopadhyay, B., E. F. Johnson, and R. S. Wolfe.** 2000. A novel pH2 control on the expression of flagella in the hyperthermophilic strictly hydrogenotrophic methanarchaeaon *Methanococcus jannaschii*. Proc. Natl. Acad. Sci. USA **97:**11522–11527.
29. **Oostergetel, G. T., W. Keegstra, and A. Brisson.** 1998. Automation of specimen selection and data acquisition for protein electron crystallography. Ultramicroscopy **74:**47–59.
30. **Paggi, R. A., C. B. Martone, C. Fuqua, and R. E. De Castro.** 2003. Detection of quorum sensing signals in the haloalkaliphilic archaeon Natronococcus occultus. FEMS Microbiol. Lett. **221:**49–52.
31. **Patenge, N., A. Berendes, H. Engelhardt, S. C. Schuster, and D. Oesterhelt.** 2001. The fla gene cluster is involved in the biogenesis of flagella in *Halobacterium salinarum*. Mol. Microbiol. **41:**653–663.
32. **Peabody, C. R., Y. J. Chung, M. R. Yen, D. Vidal-Ingigliardi, A. P. Pugsley, and M. H. Saier, Jr.** 2003. Type II protein secretion and its relationship to bacterial type IV pili and archaeal flagella. Microbiology **149:**3051–3072.
33. **Schelert, J., V. Dixit, V. Hoang, J. Simbahan, M. Drozda, and P. Blum.** 2004. Occurrence and characterization of mercury resistance in the hyperthermophilic archaeon *Sulfolobus solfataricus* by use of gene disruption. J. Bacteriol. **186:**427–437.
34. **She, Q., R. K. Singh, F. Confalonieri, Y. Zivanovic, G. Allard, M. J. Awayez, C. C. Chan-Weiher, I. G. Clausen, B. A. Curtis, A. De Moors, G. Erauso, C. Fletcher, P. M. Gordon, I. Heikamp-de Jong, A. C. Jeffries, C. J. Kozera, N. Medina, X. Peng, H. P. Thi-Ngoc, P. Redder, M. E. Schenk, C. Theriault, N. Tolstrup, R. L. Charlebois, W. F. Doolittle, M. Duguet, T. Gaasterland, R. A. Garrett, M. A. Ragan, C. W. Sensen, and J. van der Oost.** 2001. The complete genome of the crenarchaeon *Sulfolobus solfataricus* P2. Proc. Natl. Acad. Sci. USA **98:**7835–7840.
35. **Sundberg, S. A., M. Alam, M. Lebert, J. L. Spudich, D. Oesterhelt, and G. L. Hazelbauer.** 1990. Characterization of *Halobacterium halobium* mutants defective in taxis. J. Bacteriol. **172:**2328–2335.
36. **Szabó, Z., S. V. Albers, and A. J. M. Driessen.** 2006. Active-site residues in the type IV prepilin peptidase homologue PibD from the archaeon *Sulfolobus solfataricus*. J. Bacteriol. **188:**1437–1443.
37. **Thomas, N. A., S. L. Bardy, and K. F. Jarrell.** 2001. The archaeal flagellum: a different kind of prokaryotic motility structure. FEMS Microbiol. Rev. **25:**147–174.
38. **Thomas, N. A., and K. F. Jarrell.** 2001. Characterization of flagellum gene families of methanogenic archaea and localization of novel flagellum accessory proteins. J. Bacteriol. **183:**7154–7164.
39. **Thomas, N. A., S. Mueller, A. Klein, and K. F. Jarrell.** 2002. Mutants in flaI and flaJ of the archaeon *Methanococcus voltae* are deficient in flagellum assembly. Mol. Microbiol. **46:**879–887.
40. **Trachtenberg, S., V. E. Galkin, and E. H. Egelman.** 2005. Refining the structure of the *Halobacterium salinarum* flagellar filament using the iterative helical real space reconstruction method: insights into polymorphism. J. Mol. Biol. **346:**665–676.
41. **van Heel, M., M. Schatz, and E. Orlova.** 1992. Correlation functions revisited. Ultramicroscopy **46:**307–316.
42. **Weiss, R. L.** 1973. Attachment of bacteria to sulphur in extreme environments. J. Gen. Microbiol. **77:**501–507.
43. **Worthington, P., V. Hoang, F. Perez-Pomares, and P. Blum.** 2003. Targeted disruption of the α-amylase gene in the hyperthermophilic archaeon *Sulfolobus solfataricus*. J. Bacteriol. **185:**482–488.